Springer

Journal of
Mechanical
Science and
Technology

Journal of Mechanical Science and Technology 23 (2009) 1422~1427

www.springerlink.com/content/1738-494x
DOI 10.1007/s12206-008-1205-z

Pseudospectral analysis of buckling and free vibration of rectangular Mindlin plates †

Jinhee Lee*

Department of Mechanical and Design Engineering, Hongik University, Choongnam 339-701, Korea

(Manuscript Received May 19, 2008; Revised December 5, 2008; Accepted December 11, 2008)

Abstract

A study of buckling and free vibration of rectangular Mindlin plates is presented. The analysis is based on the pseudospectral method, which uses basis functions that satisfy the boundary conditions. The equations of motion are collocated to yield a set of algebraic equations that are solved for the critical buckling load and for the natural frequencies in the presence of the in-plane loads. Numerical examples of rectangular plates with SS-C-SS-C boundary conditions are provided for various aspect ratios and thickness ratios, which show good agreement with those of the classical plate theory when the thickness ratio is very small.

Keywords: Free vibration; Buckling; Eigen values; Pseudospectral method; Mindlin plates

1. Introduction

In the analyses of the buckling and free vibration of rectangular plates researchers have assumed classical plate theory and expressed the deflection as

$$w(x,y)=\sum_{k=1}^{K}\sum_{l=1}^{L}c_{kl}\phi_k(x)\varphi_l(y) \tag{1}$$

where $\phi_k(x)$ and $\varphi_l(y)$ are the characteristic beam functions satisfying the geometrical boundary conditions in the x-direction and the y-direction, respectively, and applied the Rayleigh-Ritz method [1-5].

Real plates, however, may have appreciable thickness in which case the transverse shear and the rotary inertia are not negligible as assumed in the classical plate theory. As a result, the thick plate model based on the Mindlin theory has gained popularity. Brunelle and Robertson investigated the buckling and vibration of thick, simply supported rectangular plates subject to initial stress where they derived five equations of motion and solved the characteristic equations for the buckling load and natural frequencies [6, 7]. Liew *et al.* studied the buckling behavior of rectangular Mindlin plates by applying a Levy-type solution method to the state space expression of equations of motion [8]. Liew *et al*. employed a meshfree method based on the reproducing kernel particle approximation to compute the buckling loads and the natural frequencies of rectangular and skew Mindlin plates [9].

Even though the buckling and free vibration of rectangular Mindlin plates have been studied by many researchers, it is still advantageous to have a simple and straightforward procedure to compute the buckling load and natural frequencies of Mindlin plates. The pseudospectral method can be considered as a spectral method that performs a collocation process. As the formulation is powerful enough to produce approximate solutions close to exact solutions, the pseudospectral method has been extensively used in the solution of computational physics and fluid me-

† This paper was recommended for publication in revised form by Associate Editor Eung-Soo Shin

*Corresponding author. Tel.: +82 41 860 2589, Fax.: +82 41 862 2664
E-mail address: jinhlee@hongik.ac.kr

chanic problems [10]. However, it has been largely unnoticed by the structural analysis community, and few articles are available where the pseudospectral method has been applied to the buckling and vibration analysis of plates. The present study is a continuation of the previous work [11] where the pseudospectral method was applied to a free vibration analysis of rectangular Mindlin plates which were free of in-plane loads.

2. Formulations

The equations of motion governing the buckling and free vibration of plates based on the Mindlin theory are

$$\begin{aligned}
&D\left(\frac{\partial^2\Psi_x}{\partial x^2}+\frac{1-\nu}{2}\frac{\partial^2\Psi_y}{\partial y^2}+\frac{1+\nu}{2}\frac{\partial^2\Psi_y}{\partial x\partial y}\right)\\
&\quad-\kappa Gh\left(\Psi_x+\frac{\partial W}{\partial x}\right)=\frac{\rho h^3}{12}\frac{\partial^2\Psi_x}{\partial t^2}\ ,\\
&D\left(\frac{1-\nu}{2}\frac{\partial^2\Psi_y}{\partial x^2}+\frac{\partial^2\Psi_y}{\partial y^2}+\frac{1+\nu}{2}\frac{\partial^2\Psi_x}{\partial x\partial y}\right)\\
&\quad-\kappa Gh\left(\Psi_y+\frac{\partial W}{\partial y}\right)=\frac{\rho h^3}{12}\frac{\partial^2\Psi_y}{\partial t^2}\ ,\\
&\kappa Gh\left(\frac{\partial\Psi_x}{\partial x}+\frac{\partial\Psi_y}{\partial y}+\frac{\partial^2 W}{\partial x^2}+\frac{\partial^2 W}{\partial y^2}\right)\\
&\quad=N_x\frac{\partial^2 W}{\partial x^2}+N_y\frac{\partial^2 W}{\partial y^2}+\rho h\frac{\partial^2 W}{\partial t^2}
\end{aligned}\tag{2}$$

where $D=Eh^3/12(1-\nu^2)$. Ψ_x, Ψ_y and W are the bending rotation normal to the midplane in the x-direction, the bending rotation normal to the midplane in the y-direction and the transverse displacement, respectively. E and G are Young's modulus and the shear modulus. h, κ, ν and ρ are the thickness of the plate, the shear correction factor, Poisson's ratio and the density. The size of the plate is $X\times Y$ as depicted in Fig. 1. $N_x=\alpha N_o$ and $N_y=\beta N_o$ are the uniform in-plane loads in the x-direction and in the y-direction, respectively. The dimension of N_o is force per unit length.

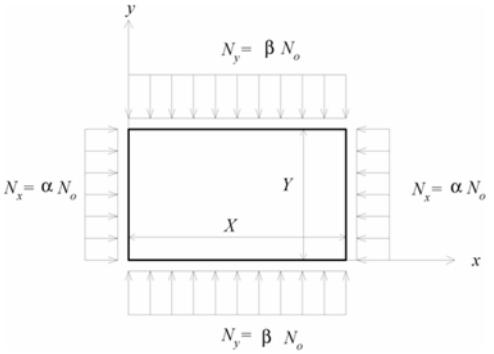

Fig. 1. Geometry of rectangular Mindlin plate and in-plane loads.

Assuming the harmonic motions in time

$$\begin{aligned}
\Psi_x(x,y,t)&=\psi_x(x,y)\sin\omega t\ ,\\
\Psi_y(x,y,t)&=\psi_y(x,y)\sin\omega t\ ,\\
W(x,y,t)&=w(x,y)\sin\omega t
\end{aligned}\tag{3}$$

and the coordinate transformation

$$\begin{aligned}
\xi&=\frac{2x}{X}-1\in[-1,1],\\
\eta&=\frac{2y}{Y}-1\in[-1,1]
\end{aligned}\tag{4}$$

Eq. (2) is rewritten as

$$\begin{aligned}
&2D\left(\frac{2}{X^2}\frac{\partial^2\psi_x}{\partial\xi^2}+\frac{1-\nu}{Y^2}\frac{\partial^2\psi_x}{\partial\eta^2}+\frac{1+\nu}{XY}\frac{\partial^2\psi_y}{\partial\xi\partial\eta}\right)\\
&\quad-\kappa Gh\left(\psi_x+\frac{2}{X}\frac{\partial w}{\partial\xi}\right)=-\omega^2\frac{\rho h^3}{12}\psi_x\ ,\\
&2D\left(\frac{1-\nu}{X^2}\frac{\partial^2\psi_y}{\partial\xi^2}+\frac{2}{Y^2}\frac{\partial^2\psi_y}{\partial\eta^2}+\frac{1+\nu}{XY}\frac{\partial^2\psi_x}{\partial\xi\partial\eta}\right)\\
&\quad-\kappa Gh\left(\psi_y+\frac{2}{Y}\frac{\partial w}{\partial\eta}\right)=-\omega^2\frac{\rho h^3}{12}\psi_y\ ,\\
&\kappa Gh\left(\frac{2}{X}\frac{\partial\psi_x}{\partial\xi}+\frac{2}{Y}\frac{\partial\psi_y}{\partial\eta}+\frac{4}{X^2}\frac{\partial^2 w}{\partial\xi^2}+\frac{4}{Y^2}\frac{\partial^2 w}{\partial\eta^2}\right)\\
&\quad=N_o\left(\frac{4\alpha}{X^2}\frac{\partial^2 w}{\partial\xi^2}+\frac{4\beta}{Y^2}\frac{\partial^2 w}{\partial\eta^2}\right)-\omega^2\rho h w
\end{aligned}\tag{5}$$

ψ_x, ψ_y and w are then approximated by series expansions:

$$\begin{aligned}
\psi_x(\xi,\eta)&=\sum_{k=1}^{K}\sum_{l=1}^{L}a_{kl}A_k(\xi)U_l(\eta)\ ,\\
\psi_y(\xi,\eta)&=\sum_{k=1}^{K}\sum_{l=1}^{L}b_{kl}B_k(\xi)V_l(\eta)\ ,\\
w(\xi,\eta)&=\sum_{k=1}^{K}\sum_{l=1}^{L}c_{kl}C_k(\xi)F_l(\eta)
\end{aligned}\tag{6}$$

Table 1. Convergence test of non-dimensional critical buckling load $N_{cr}^{*} = N_{cr}Y^2/D$ of rectangular plates (SS-C-SS-C boundary conditions, h/X =0.0005, $\alpha = 1$, $\beta = 0$, $\nu = 0.3$, $\kappa = 5/6$).

X/Y	$K \times L$					classical theory [12]
	8×8	9×9	10×10	11×11	14×14	
0.4	93.2592	93.2476	93.2476	93.2471	93.2471	93.2472
0.5	75.9161	75.9100	75.9100	75.9098	75.9098	75.9099
0.7	69.0972	69.0951	69.0951	69.0950	69.0950	69.0952

Table 2. Convergence test of non-dimensional frequency parameter $\lambda = \omega X^2\sqrt{\rho h/D}$ of a rectangular plate (SS-C-SS-C boundary condition, h/X =0.0005, Y/X =1, $N_o/N_{cr} = 0.5$, $\alpha = 1$, $\beta = 0$, $\nu = 0.3$, $\kappa = 5/6$).

	$K \times L$					classical theory [12]
	6×6	8×8	10×10	11×11	14×14	
1	21.60	21.53	21.53	21.53	21.53	21.53
2	38.84	38.71	38.71	38.71	38.71	38.71
3	67.02	66.57	66.57	66.57	66.57	66.57
4	86.80	84.61	84.14	84.12	84.12	84.12
5	105.5	86.30	86.30	86.30	86.30	86.30
6	145.2	128.0	127.6	127.6	127.6	127.6

where a_{kl}, b_{kl} and c_{kl} are the coefficients. K and L are the numbers of collocation points in the ξ–direction and in the η–direction.

The basis functions $A_k(\xi)$, $B_k(\xi)$, $C_k(\xi)$, $U_l(\eta)$, $V_l(\eta)$ and $F_l(\eta)$ are selected to satisfy the boundary conditions. An SS-C-SS-C rectangular plate, for example, has the following boundary conditions:

(a) simply supported (SS) at $\xi = \pm 1$:

$$\frac{\partial \psi_x}{\partial x} + \nu \frac{\partial \psi_y}{\partial y} = 0, \quad \psi_y = 0, \quad w = 0 \tag{7}$$

(b) clamped (C) at $\eta = \pm 1$:

$$\psi_x = 0, \quad \psi_y = 0, \quad w = 0 \tag{8}$$

The basis functions $A_k(\xi)$, $B_k(\xi)$ and $C_k(\xi)$ are chosen so that they satisfy the simply supported boundary conditions [11]:

$$\begin{aligned}
A_{2p-1}(\xi) &= T_{2p}(\xi) - T_0(\xi) - 2p^2\xi^2 \ , \\
A_{2p}(\xi) &= T_{2p+1}(\xi) - T_1(\xi) - \frac{4p}{p+1}\xi \ , \\
B_{2p-1}(\xi) &= T_{2p}(\xi) - T_0(\xi) \ , \\
B_{2p}(\xi) &= T_{2p+1}(\xi) - T_1(\xi) \ , \\
C_{2p-1}(\xi) &= T_{2p}(\xi) - T_0(\xi) \ , \\
C_{2p}(\xi) &= T_{2p+1}(\xi) - T_1(\xi) \ , \\
&\quad (p = 1,\ 2,\ \cdots)
\end{aligned} \tag{9}$$

$T_n(\xi)$ is the Chebyshev polynomial of the first kind defined as

$$T_n(\xi) = T_n(\cos\phi) = \cos n\phi \ , \quad (-1 \le \xi \le 1) \tag{10}$$

The basis functions $U_l(\eta)$, $V_l(\eta)$ and $F_l(\eta)$ are chosen to satisfy the clamped boundary conditions:

$$\begin{aligned}
U_{2q-1}(\eta) &= T_{2q}(\eta) - T_0(\eta) \ , \\
U_{2q}(\eta) &= T_{2q+1}(\eta) - T_1(\eta) \ , \\
V_{2q-1}(\eta) &= T_{2q}(\eta) - T_0(\eta) \ , \\
V_{2q}(\eta) &= T_{2q+1}(\eta) - T_1(\eta) \ , \\
F_{2q-1}(\eta) &= T_{2q}(\eta) - T_0(\eta) \ , \\
F_{2q}(\eta) &= T_{2q+1}(\eta) - T_1(\eta) \ , \\
&\quad (q = 1,\ 2,\ \cdots)
\end{aligned} \tag{11}$$

Substituting Eq. (6) into Eq. (5) and setting the residuals equal to zero at the Gauss-Lobatto collocation points (ξ_i, η_j), where ξ_i and η_j are given by

$$\xi_i = -\cos\frac{\pi(2i-1)}{2K}, \ \eta_j = -\cos\frac{\pi(2j-1)}{2L}, \quad (i = 1,\ 2, \cdots, K), \ (j = 1,\ 2, \cdots, L) \tag{12}$$

yields

$$\sum_{k=1}^{K}\sum_{l=1}^{L}\Bigg[a_{kl}\Bigg\{\frac{2}{X^2}A_k''(\xi_i)U_l(\eta_j)+\frac{1-\nu}{Y^2}A_k(\xi_i)U_l^{**}(\eta_j) -\frac{\kappa Gh}{2D}A_k(\xi_i)U_l(\eta_j)\Bigg\}+b_{kl}\frac{1+\nu}{XY}B_k'(\xi_i)V_l^{*}(\eta_j) -c_{kl}\frac{\kappa Gh}{DX}C_k'(\xi_i)F_l(\eta_j)\Bigg]=-\omega^2\frac{\rho h^3}{24D}\sum_{k=1}^{K}\sum_{l=1}^{L}a_{kl}A_k(\xi_i)U_l(\eta_j),$$

$$\sum_{k=1}^{K}\sum_{l=1}^{L}\Bigg[a_{kl}\frac{1+\nu}{XY}A_k'(\xi_i)U_l^{*}(\eta_j)+b_{kl}\Bigg\{\frac{1-\nu}{X^2}B_k''(\xi_i)V_l(\eta_j) +\frac{2}{Y^2}B_k(\xi_i)V_l^{**}(\eta_j)-\frac{\kappa Gh}{2D}B_k(\xi_i)V_l(\eta_j)\Bigg\} -c_{kl}\frac{\kappa Gh}{DY}C_k(\xi_i)F_l^{*}(\eta_j)\Bigg]=-\omega^2\frac{\rho h^3}{24D}\sum_{k=1}^{K}\sum_{l=1}^{L}b_{kl}B_k(\xi_i)V_l(\eta_j), \quad (13)$$

$$\sum_{k=1}^{K}\sum_{l=1}^{L}\Bigg[\frac{a_{kl}}{X}A_k'(\xi_i)U_l(\eta_j)+\frac{b_{kl}}{Y}B_k(\xi_i)V_l^{*}(\eta_j) +c_{kl}\Bigg\{\frac{2}{X^2}C_k''(\xi_i)F_l(\eta_j)+\frac{2}{Y^2}C_k(\xi_i)F_l^{**}(\eta_j)\Bigg\}\Bigg] =\frac{2N_o}{\kappa Gh}\sum_{k=1}^{K}\sum_{l=1}^{L}c_{kl}\Bigg\{\frac{\alpha}{X^2}C_k''(\xi_i)F_l(\eta_j)+\frac{\beta}{Y^2}C_k(\xi_i)F_l^{**}(\eta_j)\Bigg\} -\omega^2\frac{\rho}{2\kappa G}\sum_{k=1}^{K}\sum_{l=1}^{L}c_{kl}C_k(\xi_i)F_l(\eta_j)$$

where $'$ and $*$ are the differentiations with respect to ξ and η, respectively. Eq. (13) can be written in the matrix form as

$$[\mathbf{H}]\{\delta\}=\omega^2[\mathbf{M}]\{\delta\}+N_o[\mathbf{P}]\{\delta\} \quad (14)$$

where the vector $\{\delta\}$ is defined as

$$\{\delta\}=\{a_{11}\ a_{12}\cdots a_{KL}\ b_{11}\ b_{12}\cdots b_{KL}\ c_{11}\ c_{12}\cdots c_{KL}\}^T \quad (15)$$

The algebraic equation Eq. (14) is solved for N_o or ω, and the solution yields the estimates for the buckling loads and the natural frequencies in the presence of the in-plane loads.

3. Numerical examples and discussions

Convergence tests of the buckling loads of rectangular plates and the natural frequencies of a plate in the presence of in-plane loads are carried out and the results are given in Tables 1-2. The boundary conditions of the plates are SS-C-SS-C and the thickness ratio h/X of the plates is very small. The notations $\alpha=1$ and $\beta=0$ stand for $N_x=N_o$ and $N_y=0$, respectively. Tables 1-2 show that the convergence of the critical buckling loads for X/Y =0.4, 0.5, 0.7 is achieved for six significant figures with $K\times L=11\times11$ and that the convergence of the natural frequencies is achieved for the first six modes and for four significant figures with $K\times L=11\times11$. In Tables 1-2 the buckling loads and the natural frequencies based on the classical plate theory and the differential quadrature method [12] are also given for comparison, which are in excellent agreement with those of present study.

The critical buckling loads of SS-C-SS-C rectangular plates are computed for various aspect ratio Y/X and for various thickness ratio h/X and the results are given in Table 3, where they are compared with those of commercial finite element program ANSYS. It is shown in Table 3 that the results of the present study are in good agreement with those of the finite element method. It is also shown that the non-dimensional critical buckling load $N_{cr}^*=N_{cr}X^2/D$ decreases as either the aspect ratio Y/X or the thickness ratio h/X increases. N_{cr}^* decreases more slowly as h/X increases for a larger Y/X.

The fundamental frequencies of SS-C-SS-C rectangular plates are computed for Y/X =1 and for different thickness ratio h/X and different in-plane load ratio N_o/N_{cr}, and the results are given in Table 4. It is readily seen from Table 4 that the non-dimensional fundamental frequency $\lambda=\omega X^2\sqrt{\rho h/D}$ decreases rapidly as N_o/N_{cr} increases; however, λ changes less sensitively as h/X varies.

The numerical examples discussed so far are based on the SS-C-SS-C boundary conditions. The basis functions that satisfy the clamped boundary conditions at one edge (ξ =-1) and simply supported boundary conditions at another (ξ =1) are

$$\begin{aligned}
A_{2p-1}(\xi)&=T_{2p}(\xi)-T_0(\xi)-4p^2\xi(\xi+1)/3\ ,\\
A_{2p}(\xi)&=T_{2p+1}(\xi)-T_1(\xi)-4p(p+1)\xi(\xi+1)/3\ ,\\
B_{2p-1}(\xi)&=T_{2p}(\xi)-T_0(\xi)\ ,\\
B_{2p}(\xi)&=T_{2p+1}(\xi)-T_1(\xi)\ ,\\
C_{2p-1}(\xi)&=T_{2p}(\xi)-T_0(\xi)\ ,\\
C_{2p}(\xi)&=T_{2p+1}(\xi)-T_1(\xi)\ ,\\
&(p=1,\ 2,\ \cdots)\ .
\end{aligned} \quad (16)$$

Table 3. Non-dimensional critical buckling load $N_{cr}^{*} = N_{cr}X^2/D$ (SS-C-SS-C boundary conditions, $K \times L = 14 \times 14$, $\nu = 0.3$, $\kappa = 5/6$).

		$\alpha = 1$, $\beta = 0$				
	Y/X	h/X				
		0.001	0.005	0.01	0.05	0.1
present study	0.5	275.207	274.714	273.196	233.962	166.006
	0.7	141.503	141.376	140.984	129.847	105.437
	1	75.9083	75.8684	75.7448	72.0842	63.0039
	1.5	30.5806	30.5745	30.5554	29.9668	28.3091
	2	18.9774	18.9749	18.9671	18.7250	18.0211
FEM	0.5	275.260	274.651	273.284	233.976	125.329
	0.7	141.447	141.331	140.988	129.852	105.438
	1	75.8885	75.8485	75.7477	72.0877	63.0302
	1.5	30.5705	30.5637	30.5465	29.9689	28.3090
	2	18.9724	18.9702	18.9626	18.7256	18.0213
		$\alpha = 0$, $\beta = 1$				
	Y/X	h/X				
		0.001	0.005	0.01	0.05	0.1
present study	0.5	179.494	179.289	178.653	160.523	122.170
	0.7	103.924	103.861	103.665	97.7885	83.2251
	1	66.5517	66.5304	66.4638	64.4144	58.8011
	1.5	53.0456	53.0358	53.0052	52.0422	49.1927
	2	47.8390	47.8293	47.7989	46.8485	44.1185
FEM	0.5	179.427	179.254	178.728	160.542	122.206
	0.7	103.892	103.836	103.675	97.7995	83.2475
	1	66.5301	66.5106	66.4548	64.4158	58.8173
	1.5	53.0330	53.0248	52.9904	52.0473	49.2033
	2	47.8198	47.8103	47.7837	46.8520	44.1212

Table 4. Non-dimensional fundamental frequency parameter $\lambda = \omega X^2\sqrt{\rho h/D}$ (SS-C-SS-C boundary conditions, $K \times L = 14 \times 14$, $Y/X = 1$, $\nu = 0.3$, $\kappa = 5/6$).

	h/X	N_{cr}^{*}	N_o/N_{cr}				
			0.1	0.3	0.5	0.7	0.9
$\alpha = 1$ $\beta = 0$	0.005	75.8684	27.62	24.76	21.53	17.71	12.80
	0.01	75.7448	27.60	24.75	21.51	17.70	12.80
	0.02	75.2583	27.53	24.68	21.47	17.68	12.80
	0.05	72.0842	27.03	24.27	21.15	17.48	12.80
	0.1	63.0039	25.49	22.96	20.12	16.80	12.63
$\alpha = 0$ $\beta = 1$	0.005	66.5304	27.52	24.39	20.73	16.16	9.404
	0.01	66.4638	27.50	24.38	20.72	16.15	9.399
	0.02	66.1994	27.43	24.31	20.67	16.12	9.379
	0.05	64.4144	26.93	23.89	20.33	15.87	9.247
	0.1	58.8011	25.39	22.58	19.26	15.10	8.843

The procedures to form the basis functions of Eq. (9), Eq. (11) and Eq. (16) are explained in the previous work [11], and one can build basis functions for boundary conditions such as SS-SS-SS-SS, SS-SS-SS-C, SS-SS-C-C, SS-C-C-C and C-C-C-C with ease.

4. Conclusions

A pseudospectral method is applied to the analysis of the buckling and the free vibration of rectangular plates based on the Mindlin theory. The bending rotations and the transverse displacement are approxi-

mated by the series expansions of Chebyshev polynomials that have been tailored to satisfy the boundary conditions. The governing equations of motion are collocated to yield a set of algebraic equations that are solved for the critical buckling load and for the natural frequencies in the presence of the in-plane loads. Numerical examples are provided for the SS-C-SS-C boundary conditions, which show good agreement with those of the classical plate theory when the thickness ratio is very small. Numerical examples also include results of the buckling load and the natural frequencies of rectangular plates for various aspect ratios and thickness ratios. The present study offers a simple and straightforward procedure for the computation of the critical buckling load and the natural frequencies of rectangular Mindlin plates.

References

[1] S. F. Bassily and S. M. Dickinson, Buckling and lateral vibration of rectangular plates subject to in-plane loads-a Ritz approach, *Journal of Sound and Vibration*, 24(2) (1972) 219-239.

[2] S. F. Bassily and S. M. Dickinson, Buckling and vibration of in-plane loaded plates treated by a unified Ritz approach, *Journal of Sound and Vibration*, 59(1) (1978) 1-24.

[3] S. M. Dickinson, The buckling and frequency of flexural vibration of rectangular isotropic and orthotropic plates using Rayleigh's method, *Journal of Sound and Vibration*, 61(1) (1978) 1-8.

[4] M. M. Kaldas and S. M. Dickinson, Vibration and buckling calculations for rectangular plates subject to complicated in-plane stress distributions by using numerical integration in a Rayleigh-Ritz analysis, *Journal of Sound and Vibration*, 75(2) (1981) 151-162.

[5] D. J. Mead, Vibration and buckling of flat free-free plates under non-uniform in-plane thermal stresses, *Journal of Sound and Vibration*, 260 (2003) 141-165.

[6] E. J. Brunelle and S. R. Robertson, Initially stressed Mindlin plates, *American Institute of Aeronautics and Astronautics Journal*, 12 (1974) 1036-1045.

[7] E. J. Brunelle and S. R. Robertson, Vibrations of an initially stressed thick plate, *Journal of Sound and Vibration*, 45(3) (1976) 405-416.

[8] K. M. Liew, Y. Xiang and S. Kitipornchai, Analytical buckling solutions for Mindlin plates involving free edges, *International Journal of Mechanical Sciences*, 38(10) (1996) 1127-1138.

[9] K. M. Liew, J. Wang, T. Y. Ng and M. J. Tan, Free vibration and buckling analyses of shear-deformable plates based on FSDT meshfree method, *Journal of Sound and Vibration*, 276 (2004) 997-1017.

[10] J. P. Boyd, *Chebyshev & Fourier Spectral Methods, Lecture Notes in Engineering* 49, Springer-Verlag, 1989.

[11] J. Lee, Eigenvalue analysis of rectangular Mindlin plates by Chebyshev pseudospectral method, *International Journal of Korean Society of Mechanical Engineers*, 17 (2003) 370-379.

[12] X. Wang, L. Gan and Y. Wang, A differential quadrature analysis of vibration and buckling of an SS-C-SS-C rectangular plate loaded by linearly varying in-plane stresses, *Journal of Sound and Vibration*, 298 (2006) 420-431.

Jinhee Lee received B.S. and M.S. degrees from Seoul National University and KAIST in 1982 and 1984, respectively. He received his Ph.D. degree from the University of Michigan, Ann Arbor in 1992 and joined the Dept. of Mechanical and Design Engineering of Hongik University in Choongnam, Korea. His research interests include inverse problems, pseudospectral method, vibration and dynamic systems.